PHYSICAL REVIEW B VOLUME 32, NUMBER 9 1 NOVEMBER 1985

Hyperfine-magnetic-field measurements in the Heusler alloy Ni_2MnGa

S. Jha and H. M. Seyoum*
Department of Physics, University of Cincinnati, Cincinnati, Ohio 45221

M. de Marco
Department of Physics, State University College, Buffalo, New York 14222

G. M. Julian
Department of Physics, Miami University, Oxford, Ohio 45056

G. K. Shenoy
Solid State Division, Argonne National Laboratory, Argonne, Illinois 60439

R. A. Dunlap
Department of Physics, Dalhousie University, Halifax, Nova Scotia B3H 3J5, Canada
(Received 25 June 1985)

Time-differential perturbed-angular-correlation measurements and Mössbauer-effect measurements have been made on the Heusler alloy Ni_2MnGa. The magnitude and sign of the magnetic field extrapolated to 0 K at ^{119}Sn at the Ga site, ^{111}Cd at the Ni and Ga sites, and ^{99}Ru at the Ni site have been measured. The ^{119}Sn field was found to be +38 kOe, the ^{111}Cd field at Ni was 310 kOe and at Ga it was −228 kOe, and the ^{99}Ru field was −188 kOe. These results are discussed in terms of oscillations in the conduction-electron polarization.

INTRODUCTION

The Heusler alloys X_2MnZ where X = Ni, Cu, Pd, or Au and Y = Al, Ga, Ge, In, Sn, Sb, or Pb are of the cubic $L2_1$ structure and are mostly ferromagnetic with the moments residing entirely on the Mn atoms. As the interatomic distances between moments are sufficiently large, it is commonly believed that the magnetic properties are dominated by sinusoidal oscillations of the conduction-electron polarization.[1,2] The measurement of magnetic hyperfine fields on probes of different ionic charge located at different substitutional sites has proved a stringent test of models to explain the magnetic properties of these alloys.

Ni_2MnGa possess a well-ordered $L2_1$ structure and can accommodate a variety of probe atoms. For these reasons it is a convenient Heusler host in which to investigate hyperfine magnetic fields. Khoi, Veillet, and Campbell[3,4] have used NMR to measure fields at Ni, Mn, and Ga sites in this alloy. Also, Campbell[5] has investigated the field at Sn on the Ga site, using the Mossbauer effect.

In this work we have measured Sn, Cd, and Ru hyperfine fields at impurity sites in Ni_2MnGa. Some aspects of this work have been reported previously in preliminary form.[6,7]

EXPERIMENTAL METHODS

Samples were prepared by the method described by Webster.[8] For Mössbauer measurements the samples had 2 at.% of the Ga replaced by enriched ^{119}Sn.

For measurement of the ^{99}Ru field the alloy was doped with a small quantity of 15-day half-life ^{99}Rh on the Ni sites. The activity was prepared by the bombardment of metallic Rh with 55-MeV protons.

Measurement of the ^{111}Cd field at the Ga site was performed on samples doped with either a small quantity of carrier-free ^{111}In obtained from New England Nuclear or with $In^{111}In$ obtained by 55-MeV proton irradiation of indium metal. All proton irradiations were performed at the Indiana University Cyclotron Facility.

To measure the ^{111}Cd field at the Ni site a small quantity of the Ni was replaced by ^{111}Ag. This measurement was performed by neutron irradiation of enriched ^{110}Pd at the Research Reactor Facility of the University of Missouri.

Radioisotopes were introduced into the samples by heating for 10 min at 1100 °C under an argon atmosphere. This was followed by grinding and annealing *in vacuo* at 900 °C for 3 to 5 days.

Mössbauer-effect measurements were made at 4.2 K and at room temperature using a conventional spectrometer and a $Ca^{119m}SnO_3$ source. Also, room-temperature measurements were made in an external field of 5 kG in order to determine the sign of the hyperfine field.

Time-differential perturbed-angular-correlation (TDPAC) measurements were made using two NaI(Tl) scintillators

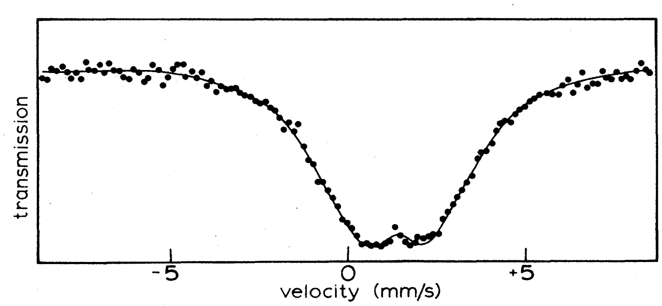

FIG. 1. ^{119}Sn Mössbauer-effect spectra obtained at 4.2 K. The computer fit is given by the solid curve.

TABLE I. Hyperfine-magnetic-field measurements in Ni_2MnGa. Unless noted, field values are from this work. Values at 0 K are extrapolated as described in the text. The number in parentheses is the error to the least significant digit. NMR denotes nuclear magnetic resonance, TDPAC, time differential angular correlations, and ME, Mössbauer effect.

Site	Probe	Method/parent	Temperature (K)	Field (kOe)
Ni	Ni	NMR	0	±125[a]
	^{99}Ru	TDPAC/^{99}Rh	293	−110(10)
			77	185 (10)
			0	188 (11)
	^{111}Cd	TDPAC/^{111}Ag	293	202 (10)
			0	310 (10)
Mn	Mn	NMR	0	−297[a]
Ga	^{69}Ga/^{71}Ga	NMR	0	−29[b]
	^{119}Sn	ME	295	+15 (5)
			4.2	38 (3)
			0	38 (3)
	^{111}Cd	TDPAC/^{111}In	333	93 (3)
			293	−160 (5)
			195	197 (4)
			77	226 (3)
			0	228 (3)

[a]Reference 3. [b]Reference 4.

coupled to RCA8575 photomultipliers fixed at 180° and conventional fast-slow coincidence circuitry. Measurements were made of the sample at various temperatures between 77 and 333 K. In randomly oriented domains the angular correlation function is given by

$$W(\theta)=1+A_2G_2(t)[P_2(\cos\theta)] \ , \tag{1}$$

where

$$G_2(t)=\tfrac{1}{5}[1+2\exp(-\delta t)\cos(\omega_2 t) + 2\exp(-\delta t)\cos(2\omega_2 t)] \tag{2}$$

and the Larmor frequency is given by

$$\omega_2=-g\mu_n H/\hbar \ . \tag{3}$$

In the above A_2 is the angular correlation anisotropy and g is the nuclear g factor. The $\exp(-\delta t)$ term accounts for damping of the perturbation and H is the hyperfine magnetic field.

The sign of the hyperfine field was determined by obtaining spectra with the counters set at 135° and the sample in an external magnetic field of 6 to 10 kG. In this case the perturbation factor was

$$G_2(t)=1+a\exp(-\delta t)\sin(2\omega_2 t) \ , \tag{4}$$

where a is the effective anisotropy. The sign of the hyperfine field was determined by the phase of the oscillations of the in-field spectrum.[9]

For ^{99}Ru measurements the 345–90-keV γ-γ cascade was utilized. In the 90-keV state, $t_{1/2}=20.7$ ns, $g=-0.284$, and $A_2=-0.13$.

The ^{111}Cd on Ga measurements made use of the 173–245-keV cascade from the ^{111}In parent. In the 245-keV state $t_{1/2}=84$ ns, $g=-0.305$, and $A_2=-0.173$. For ^{111}Cd on Ni we have used the ^{111}Ag parent and the 90–245-keV transitions; in this case, however, $A_2=-0.134$. Nuclear parameters are from Refs. 10 through 12.

RESULTS

The ^{119}Sn Mössbauer-effect spectrum obtained at 4.2 K is shown in Fig. 1. The computer fit is shown by the solid curve. This spectrum and the room-temperature spectrum

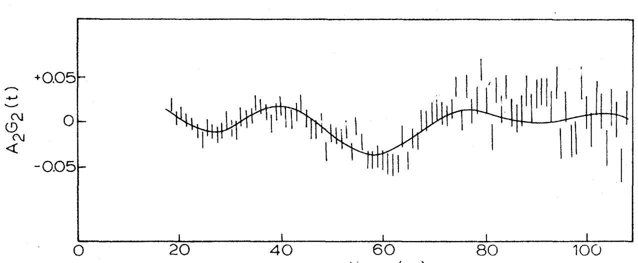

FIG. 2. ^{99}Ru TDPAC spectra obtained from the decay of ^{99}Rh on the Ni site at room temperature without an external field.

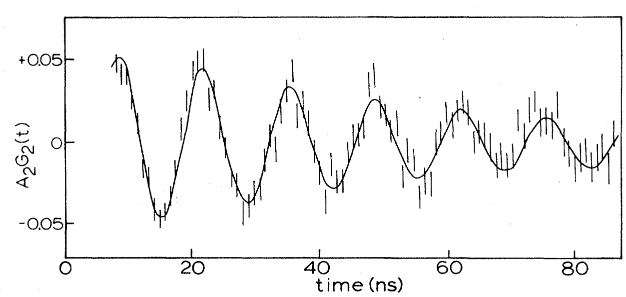

FIG. 3. ^{111}Cd TDPAC spectra obtained from the decay of ^{111}In at the Ga site at room temperature and in an externally applied field.

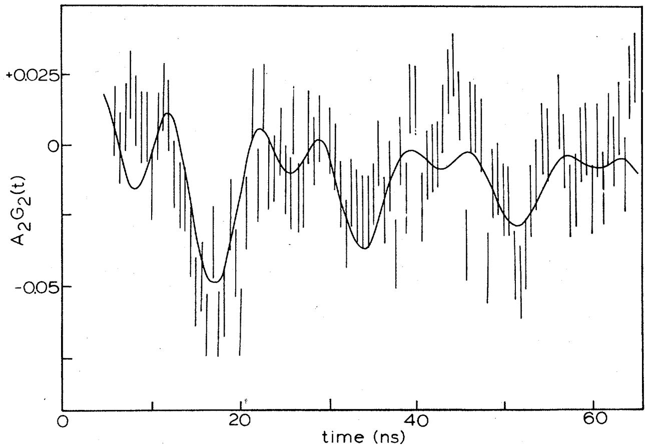

FIG. 4. Room temperature ^{111}Cd TDPAC spectra obtained from the decay of ^{111}Ag at the Ni site without an externally applied field.

were fitted to a distribution of Sn hyperfine fields, using the method of Window,[13] as previously described by Dunlap, March, and Stroink.[14] Results of these fits are given in Table I. The in-field measurement indicates that the Sn hyperfine field is positive. Previous Sn impurity Mössbauer measurements by Campbell[5] did not show any Zeeman splitting and this may have been the result of a disordered sample.

Representative TDPAC spectra are shown in Figs. 2 through 4. Computer fits to the functions described in Eqs. (1) through (4) are shown by the solid curves in the figures. Values of the hyperfine magnetic field obtained from these fits are given in Table I.

DISCUSSION

In order to properly compare various hyperfine field measurements and to consider these in the context of theoretical models, it is necessary to extrapolate measured fields to zero temperature. The validity of using the Brillouin function appropriate for spin $\frac{5}{2}$ (Mn) is illustrated by the measured ^{111}Cd field at the Ga site in Fig. 5. Table I gives values of the hyperfine field extrapolated to 0 K from the measured values and a Curie temperature of 379 K.[8] Webster[8] has reported anomalous behavior of the low-field magnetization at around 220 K. The high-field (saturation) magnetization given by Webster (8) and the hyperfine fields reported here show no such anomaly. It is generally assumed in Ni_2MnGa that the magnetic moment is confined to the Mn site; this has been measured to be $4.17\mu_B$.[8]

TABLE II. Normalized hyperfine fields h at nonmagnetic sites in Ni_2MnGa.

Site	Probe	A (kG)	H (kOe)	h (Oe/G)
Ni	Ni	2.4	±125	±52.1
	Ru	4.1	−188	−45.9
	Cd	7.2	−310	−43.1
Ga	Ga	6.2	−29	−4.68
	Sn	13	+38	+2.92
	Cd	7.2	−228	−31.7

A comparison of field values at different probe sites requires a normalization to the hyperfine field coupling constants A. Table II gives values of the zero-temperature field normalized to the values of A given by Watson and Bennett.[15] Figure 6 shows values of h, the normalized hyperfine field, as a function of effective probe valence. The Ni hyperfine field is presumed negative on the basis of Ni field systematics. The Ni valence has previously been discussed in terms of field trends in Heusler alloys and it is believed to be small.[16] As the Ru substitutes for Ni, this is probably a reasonable assumption for this probe as well. The clear trend of increasing h as a function of probe valence is observed here, as in other Heusler alloys.[17] As well, we see in Fig. 6 a distinction between the field trends at the Ni sites and those at the Ga sites. This distinction is not made in the Jena-Geldart theory[1] but is present as a result of the oscillatory behavior of the conduction band in the Blandin-Campbell theory.[2] We will look at the latter theoretical predictions in more detail.

Campbell and Blandin[2] give the polarization of the conduction band at a particular probe site due to a unit magnetic moment located at r_1 as

$$p(r_i) = (1/r_i^3)\cos[2k_F r_i + 2\delta_0 + \eta(r_0)] \ , \qquad (5)$$

where k_F is the Fermi vector. δ_0 and η are discussed below.

The hyperfine field is thus expressed as[18]

$$H = A \sum \mu(r_i) p(r_i) \ , \qquad (6)$$

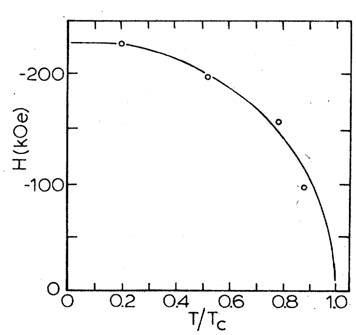

FIG. 5. Temperature dependence of the ^{111}Cd field at the Ga site. The solid curve is the Brillouin function for spin $\frac{5}{2}$.

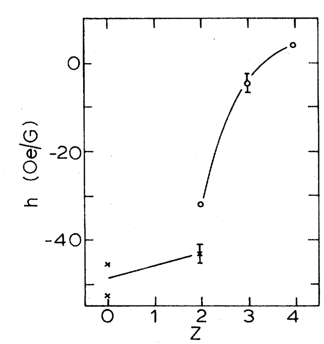

FIG. 6. Normalized hyperfine fields as a function of effective probe valence at Ni sites (×) and Ga sites (o).

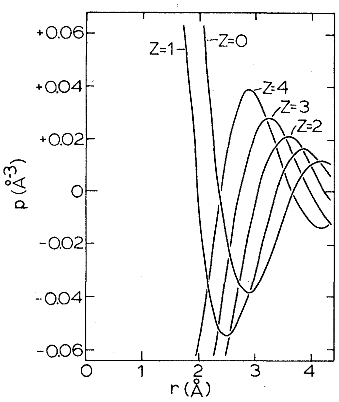

FIG. 7. Conduction-electron polarization per unit moment from Eq. (5) for different probe valences in Ni_2MnGa. The distances are measured from the magnetic Mn ion.

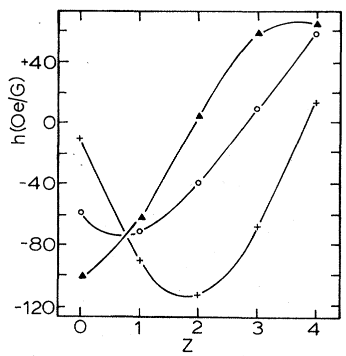

FIG. 8. Theoretical prediction for the normalized hyperfine field at Ni (+) and Ga (○) sites in Ni_2MnGa and Ni (▲) using $\eta = \pi$ at 2 nn. Values are calibrated to the measured ^{111}Cd field at the Ga site.

where A is the hyperfine coupling constant and the sum is over all neighbors. Here we have taken the free electron Fermi vector to be

$$k_F = 1/a\,(48\pi^2\eta_0)^{1/3} \ , \tag{7}$$

where a is the lattice parameter, 5.825 Å,[8] and η_0 is the contribution to the conduction band per atom. Following Dunlap, Jha, and Julian,[19] and using 4.5 spin-down electrons per Mn and 0.1 conduction electrons per Ni (16), we find $\eta_0 = 1.343$ and $k_F = 1.476$ Å^{-1}. The $2\delta_0$ term in (5) accounts for the perturbations of the conduction band due to the impurity charge Z, and is given by

$$\delta_0 = (\pi/8)(Z - \eta_0) \ . \tag{8}$$

The η term in (5) is a preasymptotic correction factor and has a radial dependence given by[2,18,20]

$$\eta(r_i) = \frac{\pi a}{4 r_i} \tag{9}$$

or $\pi/2$ for second-nearest neighbors. Figure 7 shows values of $p(r_i)$ for different probe valences in Ni_2MnGa. Because of the oscillatory nature of $p(r_i)$, as well as the growing number of neighbors per unit radius, it is necessary to consider neighbors out to about 2.5 lattice parameters in order to obtain an estimate of the hyperfine field to ~10%. Figure 7 shows the calculated $p(r_i)$ as a function of r for probes of different valences. It is clear from Fig. 7 that the trend toward positive fields for probes of higher valence comes from a shift of $p(r_i)$ for the first-few-neighbor shells from large negative values to moderate positive values. Figure 8 shows calculated values of the hyperfine field. A comparison with Fig. 6 shows that the trend predicted for the Ga-site field has been observed experimentally, although the numerical agreement is not exceptional. This has generally been the situation for *sp*-site hyperfine fields previously measured in other Heusler alloys. The trend at the Ni site, however, is not well predicted by the theory. The agreement is found to be quite good if the phase of the preasymptotic correction is taken to be π, rather than $\pi/2$, for second-nearest neighbors; see Fig. 8. We are not necessarily justified in assuming *a priori* that the preasymptotic phase correction will be the same for different sites. Additional nonmagnetic probe hyperfine fields in Ni_2MnGa would be of interest to confirm whether or not the trend shown in Fig. 6 continues to be described by the curve in Fig. 8 for $\eta = \pi$ at $r = a/2$ for different effective Z.

This work was supported by grants from the University Research Council, University of Cincinnati and the Natural Sciences and Engineering Research Council of Canada.

*Present address: Department of Physics, University of Nigeria, Nsukka, Nigeria.

[1]P. Jena and D. J. W. Geldart, J. Magn. Magn. Mater. **8**, 99 (1978).
[2]I. A. Campbell and A. Blandin, J. Magn. Magn. Mater **1**, 1 (1975).
[3]Le Dang Khoi, P. Veillet, and I. A. Campbell, J. Phys. F **8**, 1811 (1978).
[4]Le Dang Khoi, P. Veillet, and I. A. Campbell, J. Phys. F **7**, 2561 (1977).
[5]C. C. M. Campbell, J. Phys. F **5**, 1931 (1975).
[6]M. Elfazani, M. deMarco, S. Jha, G. M. Julian, and J. W. Blue, J. Appl. Phys. **52**, 2043 (1981).
[7]S. Jha, H. M. Seyoum, M. deMarco, G. M. Julian, D. A. Stubbs, J. W. Blue, M. T. X. Silva, and A. Vasquez, Hyperfine Interact. **15–16**, 685 (1983).
[8]P. J. Webster, Ph.D. thesis, University of Sheffield, 1968 (unpublished).
[9]S. Jha, H. M. Seyoum, G. M. Julian, R. A. Dunlap, A. Vasquez, J. G. M. daCunnha, and S. M. M. Ramos, Phys. Rev. B **32**, 3279 (1985).
[10]E. Matthais, S. S. Rosenblum, and D. A. Shirley, Phys. Rev. Lett. **14**, 46 (1965).
[11]R. S. Raghavan and P. Raghavan, Nucl. Instrum. Methods **92**, 435 (1971).
[12]R. M. Steffan and H. Franenfelder, in *Perturbed Angular Correlation*, edited by E. Karlsson, E. Matthais, and R. Siegbahm (North-Holland, Amsterdam, 1964).
[13]B. Window, J. Phys. E **4**, 401 (1971).
[14]R. A. Dunlap, R. H. March, and G. Stroink, Can. J. Phys. **59**, 1577 (1981).
[15]R. E. Watson and L. H. Bennett, Phys. Rev. B **15**, 502 (1977).
[16]W. R. Mayo and R. A. Dunlap, J. Appl. Phys. **53**, 8082 (1982).
[17]M. Tenhover, P. Boolchand and J. Wang, J. Magn. Magn. Mater. **20**, 158 (1980).
[18]R. A. Dunlap and D. F. Jones, Phys. Rev. B **26**, 6013 (1982).
[19]R. A. Dunlap, S. Jha, and G. M. Julian, Can. J. Phys. **62**, 396 (1984).
[20]P. Jena and D. J. W. Geldart, Phys. Rev. B **7**, 439 (1973).